Proceedings of the 28th IEEE
EMBS Annual International Conference
New York City, USA, Aug 30-Sept 3, 2006

Robust Overnight Monitoring of Human Vital Signs by a Non-contact Respiration and Heartbeat Detector

Changzhi Li, Jenshan Lin, and Yanming Xiao

Department of Electrical & Computer Engineering, University of Florida, Gainesville, Florida, 32611, USA
Email: changzhi@ufl.edu

***Abstract*—A positive answer is given to the question intrigued by our previous work reported in EMBC 2005: whether it is possible for a non-contact physiological movement detector to detect vital signs from four sides of a human body. In addition to the proof from measured data, theoretical analysis confirms the surprising advantage of detection from the back of the body. Based on this observation, a non-contact system was set up to perform overnight monitoring of vital signs using low power radio waves. Measurement data is presented and analyzed. The challenges and key technologies that improved the performance of our system for overnight monitoring are discussed.**

***Keywords*—Overnight monitoring, heartbeat, respiration, vital sign, Ka-band, non-contact, low-power, Doppler radar.**

I. Introduction

IT has been decades since microwave Doppler radar was proposed for non-contact healthcare monitoring and detection [1], such as cardiopulmonary monitoring for sleep apnea syndrome detection [2]. It may thus be used as a monitoring device of elder care technology. The non-contact approach provides benefits for easy implementation and less constraint on human activity. It also eliminates the concern of radiation safety because the transmit power is very low [3], especially in the high-frequency Ka-band system.

Despite the benefits it brings, the wide implementation of this type of non-contact physiological detectors in practical clinical applications was limited in the past years because of some practical issues: firstly, as an interesting question raised in EMBC 2005 [3], most of the previously reported systems detect respiration and heartbeat from the front of a human body [2]-[4], while it is uncertain about the performance when the monitored subject moves around and may not always face the antenna. Secondly, in practical clinical applications, it is desirable that the radar works stably for a long period of time, e.g. for hours in overnight monitoring. However, most of the systems reported were only tested for a short period of time in the range of a few seconds. The long-term performance was limited due to frequency drift and phase change during operation.

In this paper, we first report the measured data that demonstrates the feasibility of our Ka-band non-contact radar sensor detecting vital signs from four sides of a human body, explaining the reason that the heart rate accuracy is the highest when detecting from the back of the body. Based on this, we analyze the challenges for expanding the reliable working duration of our non-contact vital sign detector and introduce the improved system that overcomes difficulties. Finally, measurement data for overnight monitoring is provided and analyzed.

The system is described in Section II. Measured data from four sides of a human body is reported and analyzed in Section III. Long term overnight monitoring results and analysis are presented in Section IV.

II. System Description

The block diagram of the non-contact Ka-band physiological movement detector is illustrated in Fig. 1.

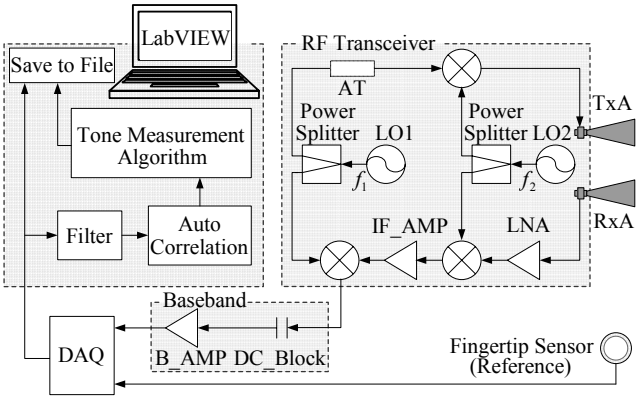

Fig. 1. System block diagram of the Ka-band non-contact physiological movement detector.

The transmitter chain contains a transmitting antenna (TxA) and an up-converter. The receiver chain includes a receiving antenna (RxA), a low noise amplifier (LNA), two down-converters, and an IF amplifier (IF_AMP). Two 3-dB power splitters are used to divide the power generated by the two local oscillators (LO1, LO2), with half of the power sent to the transmitter chain and the other half sent to the receiver chain. The output of the transmitting antenna has two main frequency components: lower sideband (LSB) $f_L = f_2 - f_1$ and upper sideband (USB) $f_U = f_2 + f_1$. The LSB and USB frequencies are 26.54 GHz and 27.66 GHz with power being either 350 μW or 14.2 μW. The power is switched from 350 μW to 14.2 μW by inserting an attenuator in the transmitter chain between the local oscillator LO1 and the up-converter.

The baseband circuit contains a DC blocker (DC_Block), and an amplifier (B_AMP). Its simple configuration,

compared to previously reported systems with baseband active filter stages [2]-[4], reduces noise, since the filtering of the low frequency (0.2~1 Hz) baseband signal requires large resistors which may introduce additional noise. The baseband filtering is then implemented in signal processing software, which also performs other functions such as auto-correlation. This filtering in software can be easily implemented and is reconfigurable.

The amplified baseband signal is digitized by a USB data acquisition module (DAQ) before sending to the laptop for signal processing. The sampling rate is 37.037 Hz. The LabVIEW program is used to process the data in real time. A sliding window of 13.824 seconds is added to the data stream to process the signal. The received signal is filtered and auto-correlated. Then, the "Tone Measurements" instrument of LabVIEW applied an advanced algorithm to pick out the signal tones of interest. This algorithm, based on the simple FFT of the received signal, uses techniques such as appropriate windowing to increase the spectral resolution. The received baseband signal as well as the calculated respiration and heartbeat rates is timely saved in data files during measurement. Therefore, the measured data can be further analyzed after the measurement is completed.

During the measurement, a wired fingertip pulse sensor (UFI_1010 pulse transducer) was attached to the subject's finger to provide the reference heartbeat.

III. Measurements From Four Sides of A Human Body

The measurement is performed from four sides of a human body seated in a chair and breathing normally, as indicated in Fig. 2. The four cases are defined as the *front*, *back*, *left*, and *right* cases. Vital signs were detected under the following combinational conditions: two power levels of 350 μW and 14.2 μW; five different distances from the antenna: 0.5 m, 1 m, 1.5 m, 2 m, and 2.5 m.

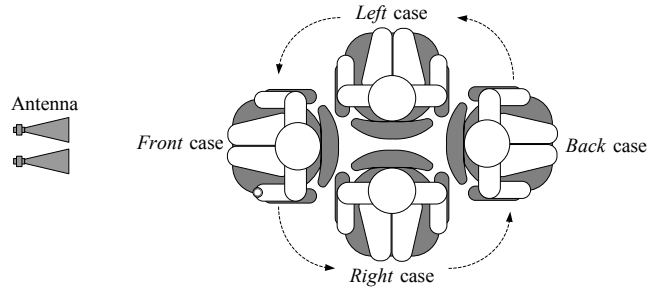

Fig. 2. Top view of the test setup for measurement from four sides of a human body.

The upper and lower limits of the acceptable detected heart rate are defined as ± 2% variation from the fingertip referenced heart rate. When the detected heart rate falls into the *confidence interval* defined by the two limits, it is considered accurate. Therefore, heart rate accuracy in a time span of 27 seconds (two times the length of the sliding window) can be calculated as the percentage of time the detected rate falls within 2% of the reference rate. The measured results of heart rate accuracy for all the above experimental conditions are listed in Table I. From any side of the body and at any of the 5 tested distances, the detection accuracy is better than 80%. The measurement in the *back* case shows the best performance, and better accuracy can be achieved with higher power.

TABLE I
Summary of Heart Rate Detection Accuracy

Distance (m)	*Front*	*Left*	*Right*	*Back*
		14.2 μW		
0.5	99.1%	96.3%	100%	97.6%
1	89.8%	89.8%	93.2%	100%
1.5	98.9%	89%	93.8%	94.3%
2	85.2%	80.5%	97.4%	93.6%
2.5	83.3%	85.7%	85.1%	85.5%
		350 μW		
0.5	100%	100%	100%	100%
1	94.8%	94.7%	93.2%	100%
1.5	98.1%	97.6%	100%	100%
2	100%	100%	100%	100%
2.5	95.1%	100%	95.2%	97.2%

The reason for better performance in the *back* case lies in the physical nature of Doppler radar detector and the characteristics of body movements due to respiration. According to [2], the received baseband signal $B(t)$ can be approximated as:

$$B(t) = \cos\left[\theta + \frac{4\pi x_r(t)}{\lambda} + \frac{4\pi x_h(t)}{\lambda} + \Delta\phi(t)\right] \qquad (1)$$

where $x_r(t)$ and $x_h(t)$ represent the body movements due to respiration and heartbeat, respectively, θ is a constant phase shift, and $\Delta\phi(t)$ is the residual phase noise. A short wavelength is desirable to increase the sensitivity to heartbeat (the $4\pi x_h(t)/\lambda$ term). This is the reason of using the Ka-band frequency. The amplitudes of $x_r(t)$ and $x_h(t)$ vary as the detection point on the body changes. In the *front* case, the amplitude of $x_h(t)$ is on the order of 0.01 mm [5], whereas $x_r(t)$ in the millimeter range has been observed, which requires $B(t)$ to be expanded as a Fourier Series with Bessel function as the coefficients [6]. Assume $x_r(t) = m\sin\omega t$ and neglect the small term related to $x_h(t)$, then:

$$\begin{aligned} B(t) &= \cos\left[\theta + \frac{4\pi m \sin(\omega t)}{\lambda} + \Delta\phi(t)\right] \\ &= \sum_{n=-\infty}^{\infty} J_n\left(\frac{4\pi m}{\lambda}\right)\cos(n\omega t + \phi) \end{aligned} \qquad (2)$$

The terms with $|n| \geq 2$ leads to harmonics of respiration in baseband signal. These harmonics due to the nonlinear Cosine transfer function, if close to heartbeat rate, desensitize the relatively small heartbeat signal and cause low detection accuracy. For example, the forth order of respiration harmonic has a frequency close to that of heartbeat signal, and causes interference on the accurate

detection when the amplitude is large. On the other hand, the amplitude of $x_r(t)$ in the *back* case is found to be comparable to that of $x_h(t)$ [7]. In this case, the problem of harmonics is significantly reduced. This is the reason for better detection accuracy in the *back* case.

IV. Overnight Monitoring

The Ka-band non-contact physiological detector system was tested for overnight monitoring of respiration and heartbeat rates. The setup of the system is shown in Fig. 3. The antenna was placed under the bed, so that for most of the time, it was transmitting RF signal toward the back of the body, which leads to the best detection accuracy as illustrated in Section III. The LabVIEW program buffers the real-time signal for the length of a sliding window (13.824 seconds), and writes the detected signals, as well as the calculated respiration and heartbeat rates into computer files every 13.824 seconds. Therefore, all the experimental data during the overnight monitoring is stored in the computer and can be analyzed by other algorithms afterwards.

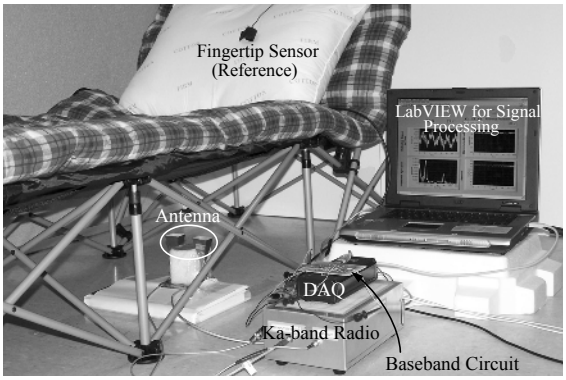

Fig. 3. Measurement setup for overnight monitoring of respiration and heartbeat rates.

For overnight measurement of sleeping subjects, the respiration and heartbeat may be weaker than in daytime. Since our system is using short wavelength in the Ka-band and has higher sensitivity than other low-frequency systems, it still achieve very good accuracy. To reduce the noise of the system, the baseband circuit was simplified as discussed in Section II, and only one low-noise operational amplifier was used to minimize added noise. Meanwhile, since larger gain may amplify the thermal noise from the resistor, the baseband gain is controlled to just overcome the quantization noise produced by the DAQ. This makes the quantization noise discernable in our detected baseband waveform. Since the desired signal is above the noise floor of the DAQ, the performance does not deteriorate.

Another important issue is the frequency and phase stability of the oscillator. Our previous work [4] has demonstrated that a drift in frequency or a burst of phase noise may change the detection point from an optimum point to a null point. For the two local oscillators used in the Ka-band radio, the high frequency one was a YIG-tuned oscillator with large tuning range from 20 GHz to 40 GHz,

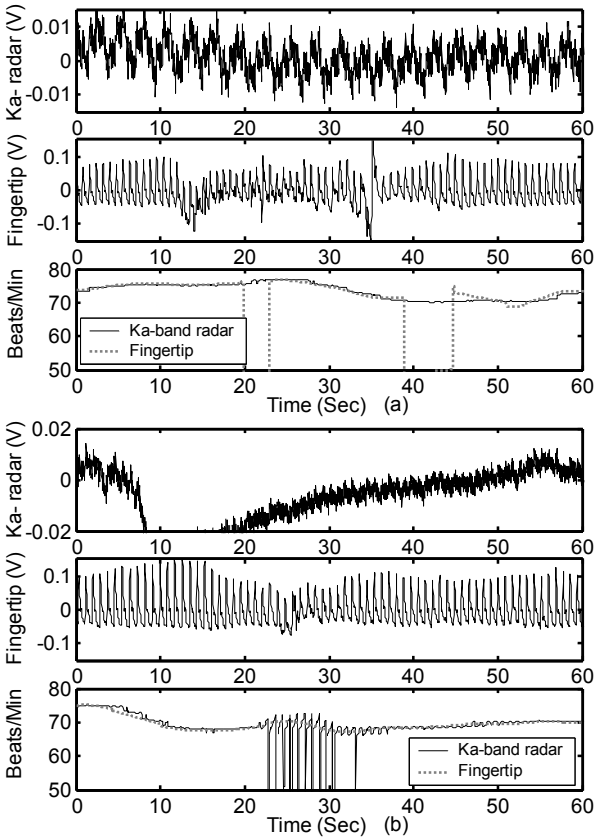

Fig. 4. One-minute measurement records when the subject's movements caused interruptions: (a) the non-contact radar was detecting normally while the fingertip sensor data shows interruptions; (b) the fingertip sensor works normally while the non-contact radar data shows interruptions.

the penalty of such a wideband oscillator is a very large phase noise and frequency drift. To eliminate this problem, an external signal generator is used to replace the YIG-tuned oscillator in the overnight measurement.

The experiments conducted were typically taken from midnight to the next morning. It is unavoidable that sometimes the subject under test may move the body during measurement. Sometimes the subject may move the finger without moving the body, in which case the non-contact detector is more likely to get an accurate rate than the fingertip measurement. Fig. 4(a) shows a one-minute record of such a case during a six-hour monitoring. On the other hand, the subject may also move the body without disturbing the fingertip, making the fingertip referenced rate more reliable, as shown in Fig. 4(b). Combining these factors, the fingertip sensor, although still used as a reference, is no longer the standard for judging the accuracy of the con-contact radar detector. Therefore, we refer the percentage of time the detected rate is within 2% of the reference rate as the *degree of agreement* of the two detection methods.

For six hours of non-interrupted monitoring, the *degree of agreement* between the non-contact radar sensor and the fingertip sensor can achieve as high as 90%. Fig. 5 shows a six-hour overnight measurement record of detected heart and respiration rates using non-contact radar detector, as well as the detected heart rate using the wired fingertip

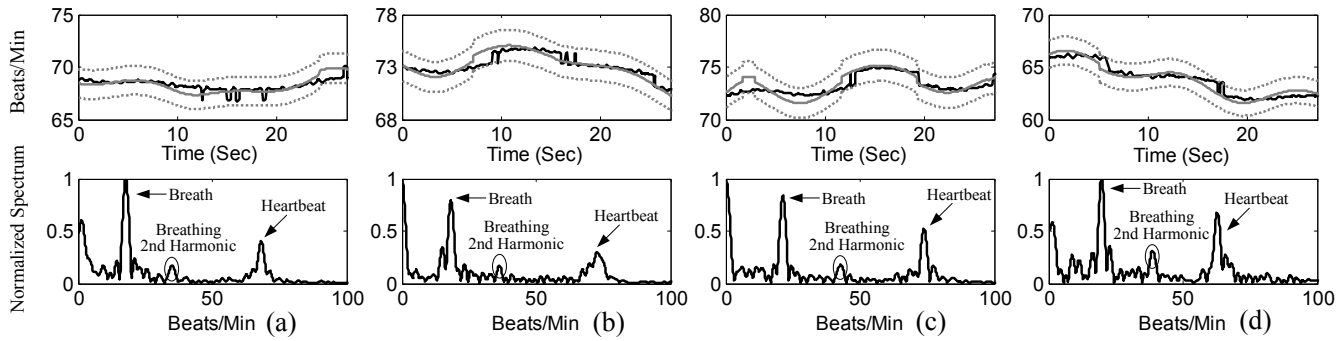

Fig. 6. 27-second heart-rate records (top), and detected baseband spectra (bottom) at t = 1hour (a), 2 hour (b), 3 hour (c), and 4 hour (d). These records correspond to Γ, Π, Λ, and Ω indicated in Fig. 5. From (a) to (d), the detection accuracy of the non-contact detector is: 100%, 99.9%, 100%, 98.63%.

sensor. In plotting these results, all the rates were running-averaged using a window size of 60 seconds. This is aimed to observe the long-term trend in rate change, and to eliminate the apparent false detections of both detected rates caused by body movement, as shown in Fig. 4. Before the running average, the *degree of agreement* between the two monitoring methods is 89.33%. By using running average with a window size of 10 seconds to eliminate apparent false detections, the *degree of agreement* achieves 92.96%.

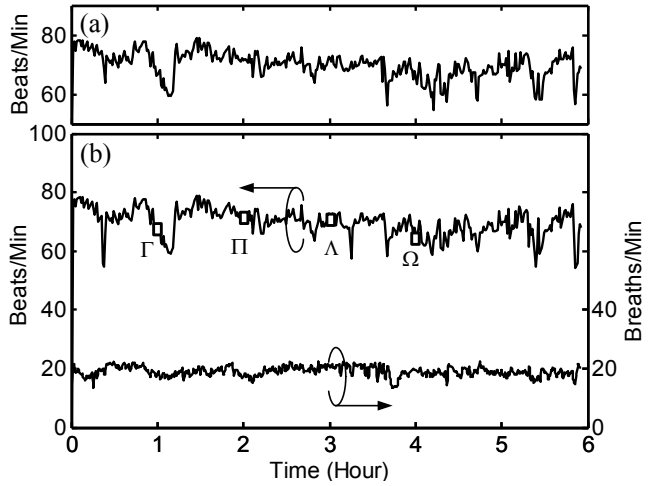

Fig. 5. Six-hour overnight measurement record of: (a) detected heart rate using wired fingertip sensor; (b) detected heart and respiration rates using non-contact radar detector;

While for the long-time monitoring, it is not practicable to use the fingertip sensor to judge the accuracy of the non-contact radar detector, we can use the fingertip sensor data to set the 2% *confidence interval* for a short period of time, provided that the heart rate detected from the fingertip is accurate. Based on this assumption, calculations of accuracy for 27 seconds at the time t = 1, 2, 3, and 4 hour are performed. These points in time correspond to the Γ, Π, Λ, and Ω points in Fig. 5. The detected heart rate compared with reference heart rate, and the baseband spectra are shown in Fig. 6. The detection accuracy at these four measurement times is: 100%, 99.9%, 100%, and 98.63% respectively. It is shown in Fig. 6 that the respiration and the heartbeat make two distinctive tones in the spectra. Meanwhile, the second order harmonic caused by respiration, discussed in Section III, are also discernable in the spectra. The interference of harmonics has been significantly reduced when the system detects the signal from the back of the body.

V. Conclusion

Based on the observation of better detection accuracy when measuring from the back of the body, as well as several improvements in the system, long-term overnight monitoring of respiration and heartbeat rates using a non-contact low-power vital sign detection system has been demonstrated. Measurement data for a consecutive six-hour period is reported. The results show that the non-contact detector is a potential alternative device, with advantages of easy implementation, no contact, and low power, for the applications of overnight monitoring of sleep apnea syndrome and irregular heartbeat needed in child and elder health care and other similar applications.

Acknowledgment

This work was partly supported by the National Science Foundation under Grant # 0421218.

References

[1] J. C. Lin, "Noninvasive microwave measurement of respiration", *Proc. of the IEEE*, vol. 63, pp. 1530-1530, Oct. 1975.

[2] A. D. Droitcour, O. Boric-Lubecke, V. M. Lubecke, J. Lin, and G. T. A. Kovac, "Range correlation and I/Q performance benefits in single-chip silicon Doppler radars for noncontact cardiopulmonary monitoring," *IEEE Trans. Microwave Theory and Techniques*, vol. 52, pp. 838-848, March 2004.

[3] Y. Xiao, J. Lin, O. Boric-Lubecke and V. M. Lubecke, "A Ka-band low power Doppler radar system for remote detection of cardiopulmonary motion," *Proc. 27th IEEE Annu. Engineering in Medicine and Biology Society Conf.*, September 1-4, 2005.

[4] Y. Xiao, J. Lin, Boric-Lubecke and V. M. Lubecke, "Frequency Tuning Technique for Remote Detection of Heartbeat and Respiration Using Low-Power Double-Sideband Transmission in Ka-Band", *IEEE Trans. Microwave Theory and Techniques*, vol. 54, May 2006.

[5] M. Singh and G. Ramachandran, "Reconstruction of Sequential Cardiac In-Plane Displacement Patterns on the Chest Wall by Laser Speckle Interferometry," *IEEE Trans. Biomed. Eng.*, vol. 38, pp. 483-489, May 1991.

[6] D. C. Champeney, *Fourier transforms and their physical applications*, Academic Press, 1973.

[7] Y. Xiao, C. Li, and J. Lin, "Accuracy of A Low-Power Ka-Band Non-Contact Heartbeat Detector Measured from Four Sides of A Human Body", *IEEE MTT-S International Microwave Symposium Digest*, June, 2006.